SUPPORTING INFORMATION

Assessing the defect tolerance of kesterite-inspired solar absorbers

Andrea Crovetto[1,2*], Sunghyun Kim[3], Moritz Fischer[4,5], Nicolas Stenger[4,5], Aron Walsh[3,6], Ib Chorkendorff[1], and Peter C. K. Vesborg[1]

[1]SurfCat, DTU Physics, Technical University of Denmark, DK-2800 Kgs. Lyngby, Denmark
[2]Department of Structure and Dynamics of Energy Materials, Helmholtz-Zentrum Berlin für Materialien und Energie GmbH, Berlin, Germany
[3]Department of Materials, Imperial College London, London SW7 2AZ, United Kingdom
[4]DTU Fotonik, Technical University of Denmark, DK-2800 Kgs. Lyngby, Denmark
[5]Center for Nanostructured Graphene (CNG), Technical University of Denmark, DK-2800 Kgs. Lyngby, Denmark
[6]Department of Materials Science and Engineering, Yonsei University, Seoul 03722, Korea
[*]E-mail: andrea.crovetto@helmholtz-berlin.de

The special case of band gap narrowing in AZTSe

In Fig. 8(a) of the main article, the calculated band gap narrowing due to the $2(I_{II} + IV_{II})$ defect cluster is plotted on the x-axis, based on the values calculated in Refs. 1, 2. The AZTSe data point is, however, a special case that needs further clarification. First, calculations of defect clusters are only available for AZTS and not for AZTSe and, second, the $2(Ag_{Zn} + Sn_{Zn})$ cluster in AZTS has a very high formation energy [2]. As a worst-case scenario, we considered the defect cluster with the largest calculated band gap narrowing among low-formation-energy defects in AZTS, which is $(Sn_{Zn} + Zn_{Sn})$. To extrapolate its band gap narrowing effect from AZTS to AZTSe we simply followed the trend of the $(Sn_{Zn} + Zn_{Sn})$ defect from CZTS to CZTSe, as shown in Ref. 1. We consider this an acceptable approximation since all four compounds have the same crystal structure (kesterite) and exhibit the same band gap trend, i.e., a band gap decrease by ∼0.5 eV when replacing S with Se.

When going from CZTS to CZTSe, the valence band upshift is reduced by a factor ∼2, and the conduction band downshift is reduced by a factor of ∼4 [1]. Using these correction factors, the calculated band gap narrowing of AZTSe is extrapolated as 70 meV, which is the value plotted on the x-axis of Fig. 8(a) in the main article for the AZTSe data point. Note that the trend identified in Fig. 8(a) is still valid if a different defect cluster is chosen for AZTSe, because all the other calculated defect clusters narrow the band gap to a smaller extent than the $(Sn_{Zn} + Zn_{Sn})$ cluster [2].

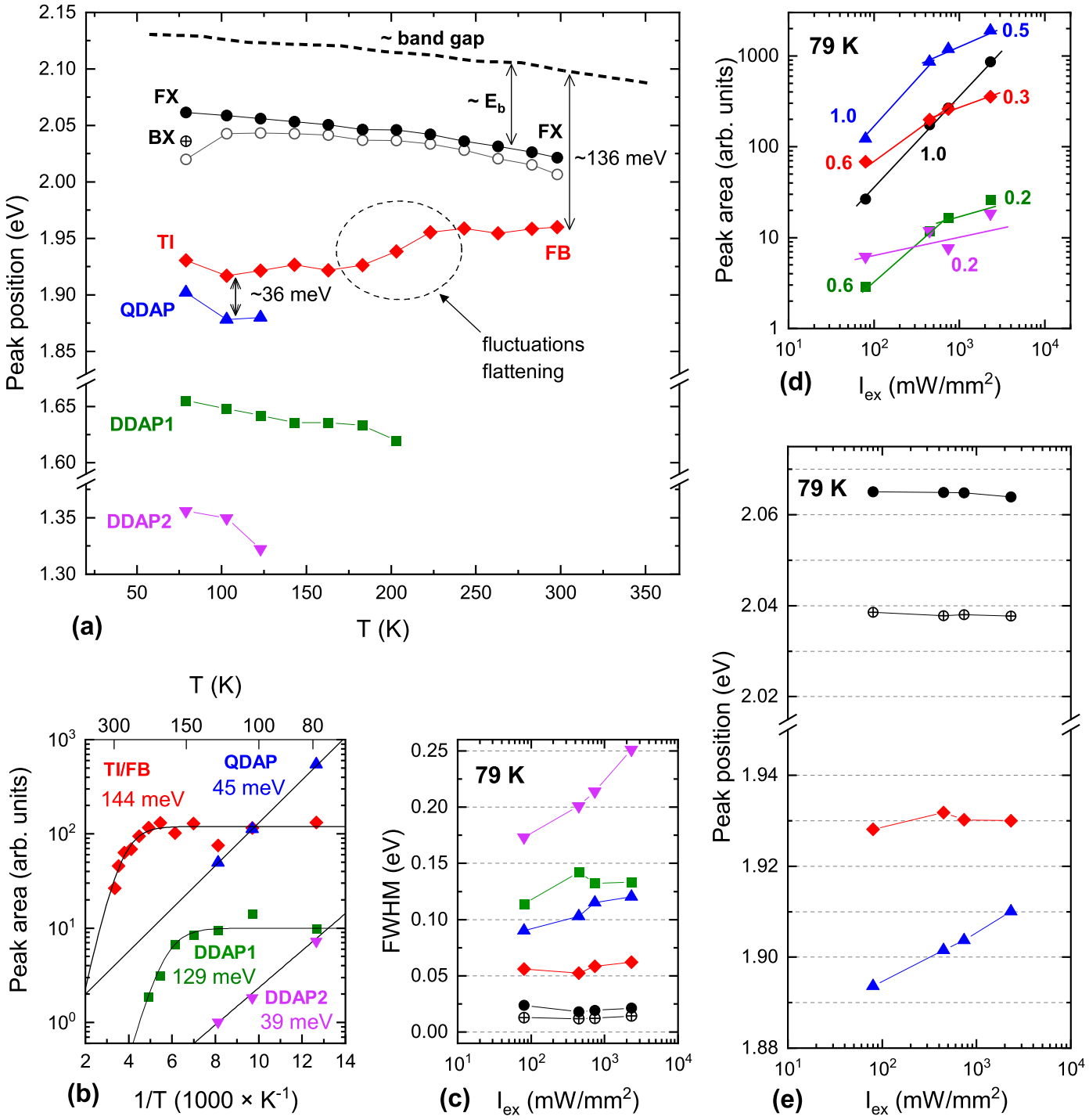

Figure S 1: Integrated area, position, and full-width at half-maximum (FWHM) of the PL peaks identified in a CBTS film as a function of temperature and excitation intensity. The parameters of each peak are obtained by least-squares fitting with a single Gaussian peak. (a): Peak position versus temperature. Each peak is labeled with the type of PL transition responsible for it. The exciton binding energy estimated from the hydrogen model, and the consequent position of the band gap energy as a function of temperature, are indicated. The temperature range corresponding to flattening of band edge fluctuations due to state filling is also indicated. (b): Arrhenius plots of PL peak areas as a function of temperature The type of transition and the fitted activation energy is indicated for each peak. (c): FWHM versus excitation intensity at 79 K. The color- and marker scheme is the same as in the previous subfigures. (d): Peak area versus excitation intensity at 79 K. The power law coefficients k under low- and high excitation are shown. (e): Peak position versus excitation intensity at 79 K. The intensity of the DDAP1 and DDAP2 peaks is too low for the small excitation-dependent positions shifts to be determined reliably.

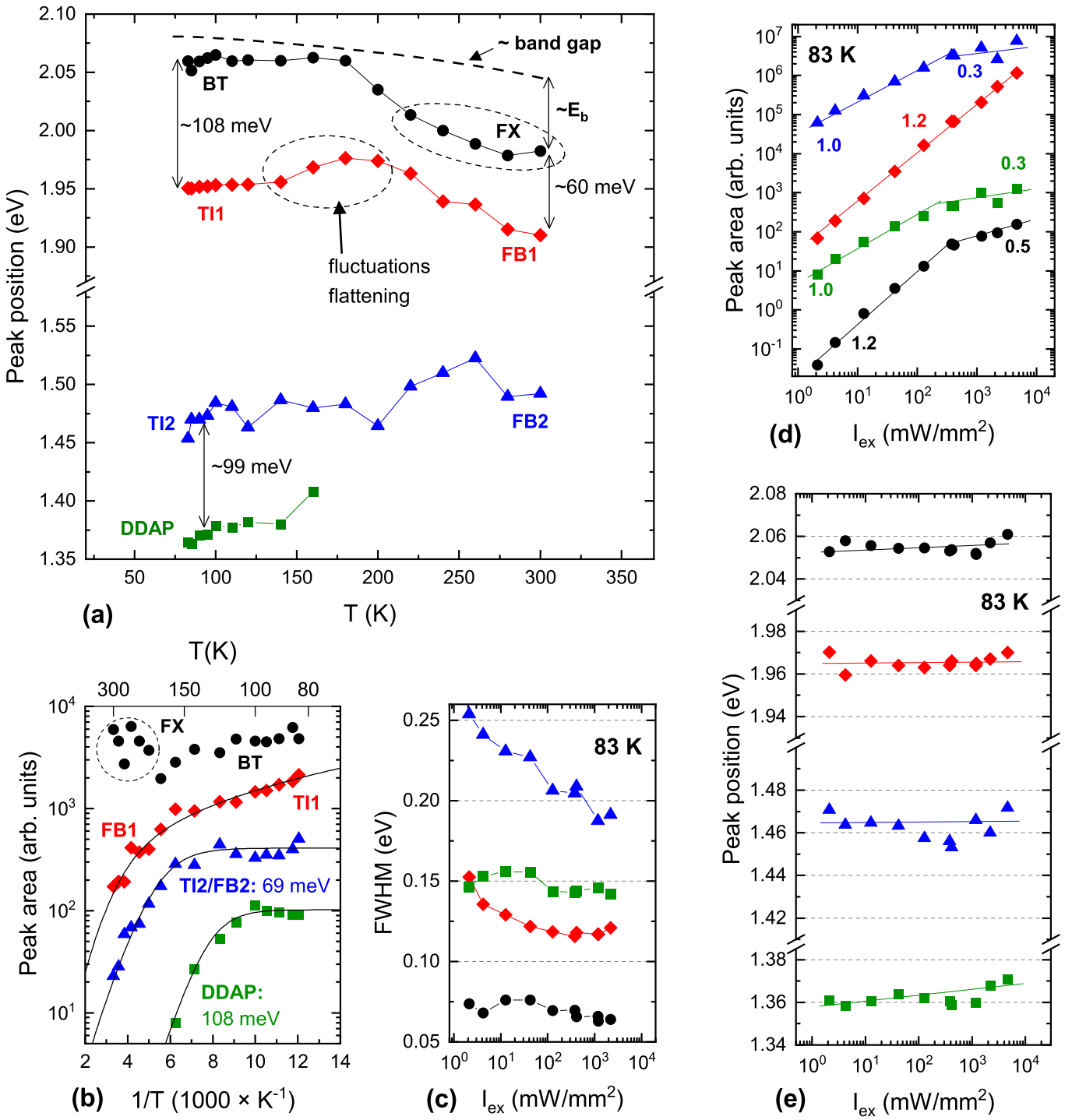

Figure S 2: Integrated area, position, and full-width at half-maximum (FWHM) of the PL peaks identified in a CSTS film as a function of temperature and excitation intensity. The parameters of each peak are obtained by least-squares fitting with a single Gaussian peak. (a): Peak position versus temperature. Each peak is labeled with the type of PL transition responsible for it. The exciton binding energy estimated from the hydrogen model, and the consequent position of the band gap energy as a function of temperature, are indicated. The temperature range corresponding to flattening of band edge fluctuations due to state filling is also indicated. (b): Arrhenius plots of PL peak areas as a function of temperature The type of transition and the fitted activation energy is indicated for each peak. (c): FWHM versus excitation intensity at 83 K. The color- and marker scheme is the same as in the previous subfigures. (d): Peak area versus excitation intensity at 83 K. The power law coefficients k under low- and high excitation are shown. (e): Peak position versus excitation intensity at 83 K.

References

[1] Chen S, Walsh A, Gong X G and Wei S H 2013 *Advanced Materials* **25** 1522–1539

[2] Yuan Z K, Chen S, Xiang H, Gong X G, Walsh A, Park J S, Repins I and Wei S H 2015 *Advanced Functional Materials* **25** 6733–6743